Journal of Applied Polymer Science

The Effect of Nonionic Monomer HAM on Properties of Cationic Surfactant-Free Acrylic/Alkyd Hybrid Emulsion

Xiaojun Shui, Yiding Shen, Guiqiang Fei, Haihua Wang, Ke Zhu

College of chemistry and chemical engineering, Key Laboratory of Auxiliary Chemistry and Technology for Chemical Industry, Ministry of Education, Shaanxi University of Science and Technology, Xi'an 710021, People's Republic of China

Correspondence to: Y. Shen (E-mail: ydshen@sust.edu.cn)

ABSTRACT: A series of cationic acrylic/alkyd resin (CPAAR) hybrid emulsions was successfully prepared through surfactant-free emulsion polymerization, using methacryloxyethyltrimethyl ammonium chloride, methyl methacrylate, butyl acrylate and alkyd resin as reaction monomers. And nonionic *N*-hydroxymethyl acrylamide (HAM) of different content was simultaneously incorporated into the CPAAR backbone. The structure of CPAAR copolymer was characterized by Fourier transform infared spectrometer, and then the effect of HAM content on properties of CPAAR emulsions was studied by particle size analyzer, transmission electron microscopy and rheometer. In addition, thermal properties, water absorption and contact angle of CPAAR latex films were also investigated. The results showed that the CPAAR emulsions prepared with 4.9 wt % HAM displayed smallest average particle size of 92.2 nm. As HAM content increased from 0 to 19.6 wt %, the initial viscosity of the emulsions increased from 22.48 to 53 mPa.s. At the same time, the emulsions transferred from Newtonian fluid to pseudoplastic fluid, and a transition from viscous liquid to elastic liquid was also detected. Meanwhile, the degradation temperature at 5% weight loss increased by 30.59°C. In addition, with increasing HAM content from 0 to 4.9 wt %, the water absorption and surface free energy of films increased by 4.42% and 5.02 mJ m^{-2}, respectively. However, the water absorption and surface free energy kept almost invariable with further increase in HAM content. © 2014 Wiley Periodicals, Inc. J. Appl. Polym. Sci. **2015**, *132*, 41406.

KEYWORDS: coatings; copolymers; crosslinking; emulsion polymerization; radical polymerization

Received 9 April 2014; accepted 14 August 2014

DOI: 10.1002/app.41406

INTRODUCTION

Waterborne coatings have received much attention because of health and environmental aspects during recent years.[1,2] Alkyd resins are polyester resins that are derived from natural oils, including soybean, sunflower and linseed oils, which are biological, polyols, and dibasic acids.[3,4] Therefore waterborne alkyd resins have been an important material choice for coatings.

Combining acrylic resin with alkyd resin has been a popular method to prepare waterborne alkyd resin coatings since the products are endowed with the advantageous of both resins. Acrylic latex coatings show short drying time, low odor and easy clean up with water.[5,6] However, penetrability of the substrate for acrylic latexes is inferior to that of alkyd emulsions, as well as the leveling property and abrasion resistance. In addition, alkyd films display higher gloss, but longer drying time. Therefore the acrylic/alkyd resins are able to overcome the disadvantages of both resins.

Waterborne acrylic/alkyd resins have been prepared through various approaches. The common approach is to polymerize acrylic monomers in the presence of an unsaturated alkyd resin through mini-emulsion polymerization.[7,8] And surfactants are usually utilized to ensure the long-term stability of acrylic/alkyd emulsions. The gloss, stain blocking and water resistance are thereby reduced since the surfactants are likely to migrate from the film bulk to the surface.[9,10] To overcome the shortcomings of surfactant, simply mixing acrylic dispersion and alkyd emulsion[11] or emulsifying alkyd with acrylic dispersion is generally adopted.[12] However, phase separation and poor stability are also accompanied with such emulsions.[13,14] Therefore, several methods are proposed to improve the compatibility between acrylic and alkyd, such as building a chemical connectivity between acrylic and alkyd. Elrebii etal.[15] prepared surfactant-free alkyd-acrylic dispersion via a condensation reaction between an acrylic prepolymer bearing carboxylic groups and a low molecular weight alkyd resin, followed by an emulsification process, which can be carried out by a simple neutralization of the carboxylic groups without addition of any surfactant. Therefore self-emulsifying acrylic/alkyd resins can be obtained by incorporating ionizable hydrophilic groups such as carboxylic groups to the acrylic/alkyd backbone.[16]

Table I. Polymerization Recipe of Cationic Acrylic/Alkyd Resin Emulsions with Different HAM Content

Sample	DMC[a]	MMA[a]	BA[a]	HAM[b] (wt %)	AR[b] (wt %)	AIBN[b] (wt %)	IPA[b] (wt %)
CPAAR0	2	10	5	0	16.7	3	5
CPAAR1	2	10	5	4.9	16.7	3	5
CPAAR2	2	10	5	9.8	16.7	3	5
CPAAR3	2	10	5	14.7	16.7	3	5
CPAAR4	2	10	5	19.6	16.7	3	5

Heretofore, most researches focus on the preparation and property of anionic waterborne acrylic/alkyd hybrids. Under the alkaline environment, the alkyd resins suffer from limited hydrolytic stability and alkali resistance. It is reported that the hydrolysis of ester bonds in anionic acrylic/alkyd hybrids under alkaline condition is a non-reversible reaction,[17–19] resulting in the decrease of molecular weight of alkyd resins.[20,21] It may greatly impair the stability of the anionic acrylic/alkyd emulsions and properties of the corresponding films.

Under such circumstance, cationic acrylic/alkyd (CPAAR) hybrid emulsions were prepared by incorporating methacryloxyethyltrimethyl ammonium chloride (DMC) and nonionic *N*-hydroxymethyl acrylamide (HAM) into the CPAAR backbone in this study. The hydrolysis of ester bonds of alkyd in weak acidic or neutral condition is more difficult than that of anionic system. Meanwhile, the dosage of neutralization agent acetic acid can de reduced through the introduction of nonionic hydrophilic HAM monomer, which is also favorable to inhibit the ester hydrolysis. In addition, the compatibility and interaction between acrylic and alkyd can be enhanced with HAM due to hydrogen bonds interaction,[22] since HAM is a kind of hydrophilic self-crosslinking monomer which possesses amino and hydroxyl groups. To our best knowledge, the preparation and properties of cationic acrylic/alkyd hybrid emulsions have been seldom reported.

The properties of waterborne acrylic/alkyd resins are largely depended on the category of acrylic monomers. In this study, a series of cationic acrylic/alkyd resin emulsions were successfully prepared by surfactant-free polymerization of acrylic monomers *in situ* in the presence of alkyd resin. Cationic monomer DMC and nonionic hydrophilic HAM are incorporated into the CPAAR backbone to obtain self-emulsifying acrylic/alkyd hybrids. Effects of nonionic monomer HAM on properties of CPAAR emulsions and films were systematically analyzed. The structure of CPAAR copolymer and thermal properties, contact angle of the CPAAR latex films were characterized by Fourier transform infrared spectroscopy (FT-IR), thermo gravimetric analysis (TGA)-differential thermogravimetry (DTG) and contact angle goniometer. And then the steady rheological properties, particle size and morphology of CPAAR dispersions were also studied with rheometry, dynamic light scattering and transmission electron microscopy (TEM).

EXPERIMENTAL

Materials

Methacryloxyethyltrimethyl ammonium chloride (DMC) was purchased from Xinyu Chemical (Jiangsu, China). Methyl methacrylate (MMA), butyl acrylate (BA), acetic acid (AC) and isopropyl alcohol (IPA) were purchased from Kemiou Chemical (Tianjing, China). Alkyd resin (AR) was purchased from Baotashan Paint (Xingping, China). *N*-hydroxymethyl acrylamide (HAM) and azodiisobutyronitrile (AIBN) were purchased from Hongyan Chemical (Tianjing, China). Deionized water was heated to 80°C in preparation of CPAAR dispersions and deionized water at room temperature was directly used for other experiments.[23]

Preparation and Experimental Mechanism of the CPAAR Emulsions

[a]m(DMC)/m(MMA)/m(BA) = 2:10:5

[b]m(HAM), m(AR), m(AIBN) and m(IPA)/m(total monomers) × 100%, respectively.

The mixture of monomers (composition of DMC, MMA, BA, HAM, and AR) and a part of IPA were first charged into a dry 500-mL three-neck round-bottom flask with reflux condenser and mechanical stirrer. Then the initiator AIBN dissolved by residual IPA was added to the reactor, followed by mechanical stirrer with a rotational speed of 500 rpm for 4 h under 80°C. After polymerization process, reaction mixture was neutralized by the same content of AC for 10 min The mixture was subsequently submitted to vigorous shear (3000 rpm) for 20 min. The process was carried out by progressively adding water. The mixture turned to a white opaque liquid at firstly forming a water-in-oil emulsion, which underwent a phase reversion forming an oil-in-water emulsion as more water was added. Then, the emulsion was further homogenized by mechanical stirring to ensure the complete emulsification process. Finally, a series of CPAAR dispersions with a solid content 30 wt % were obtained though the adjustment of HAM content over a range of 0, 4.9, 9.8, 14.7, and 19.6% and coded as CPAAR0, CPAAR1, CPAAR2, CPAAR3, and CPAAR4, respectively. The polymerization recipe, experimental scheme, and mechanism scheme of a series of CPAAR dispersions were summarized in Table I, Figure 1 and Figure 2, respectively.

As shown in Figure 2, in the preparation of acrylic/alkyd emulsion, when methacryloxyethyltrimethyl ammonium chloride, methyl methacrylate, butyl acrylate, and alkyd resin as reaction monomers were added into the flask, alkyd resin presented as chains polymer and other monomer presented as small droplets in organic solvents. With addition of azodiisobutyronitrile as initiator, radical polymerization between vinyl monomers was initiated, and then copolymers with cationic groups were thereby obtained, as shown in step 1. After 4 h, the whole monomers droplets disappeared and the more copolymers were

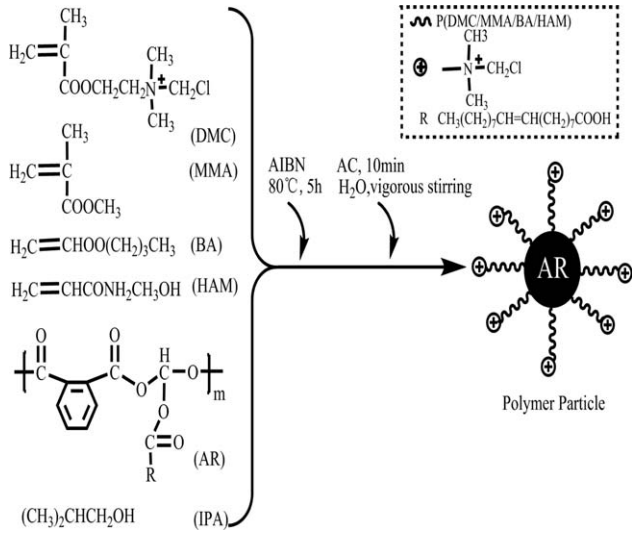

Figure 1. Experimental scheme for the preparation of CPAAR emulsions.

thereby obtained, as shown in step 2. And then the reaction mixture was neutralized and was submitted to vigorous shear to obtain small droplets of reaction mixtures, which could be easily emulsified. With the addition of water, colloidal particles began to form. To keep colloidal particle stable, hydrophilic groups tend to arrange on the surface of colloidal particles while hydrophobic groups tend to arrange in side of the colloidal particles, as shown in step 3. In a conclusion, the stability mechanism was mainly contributed by electrostatic repulsive interaction.

Film Preparation

The waterborne dispersions were cast on leveled tetrafluoroethyleneplates to allow them to dry at room temperature for 5 days and then at 60°C for 12 h. After demolding, the films were kept in a desiccator to avoid moisture.[22]

FT-IR Analysis

The infrared spectra of CPAAR copolymer was obtained on a Bruker Vector-22 spectrophotometer (Bruker, Germany) at a resolution of 4 cm^{-1}, with scanning from 4000 to 400 cm^{-1}.

Freeze-Thaw Stability of Emulsions

Emulsion samples (10 mL) were transferred into cryogenic teat tubes (internal diameter = 10 mL, height = 95 mm), which were frozen by placing them in a −20°C freezer for 22 h and then thawed by placing them in a water bath at 30°C for 2 h. If the emulsion was stable after the cycle, it was sent back to freezer for anther cycle. Between each cycle, besides observation of physical stability of the emulsion by naked eyes, particle size and zeta potential value of the emulsion was measured using particle size analyzer as an indicator of emulsion stability. Measurements were carried out in duplicates.

TG-DTG

Thermogravimetric analysis (TGA)-differential thermogravimetry (DTG) was performed in a TGA-Q500 Instrument (TA Instruments). Film samples of about 5 mg were placed in aplatinum sample pan and heated from 30 to 600°C under an N_2 atmosphere at a heating rate of 10°C min^{-1}.

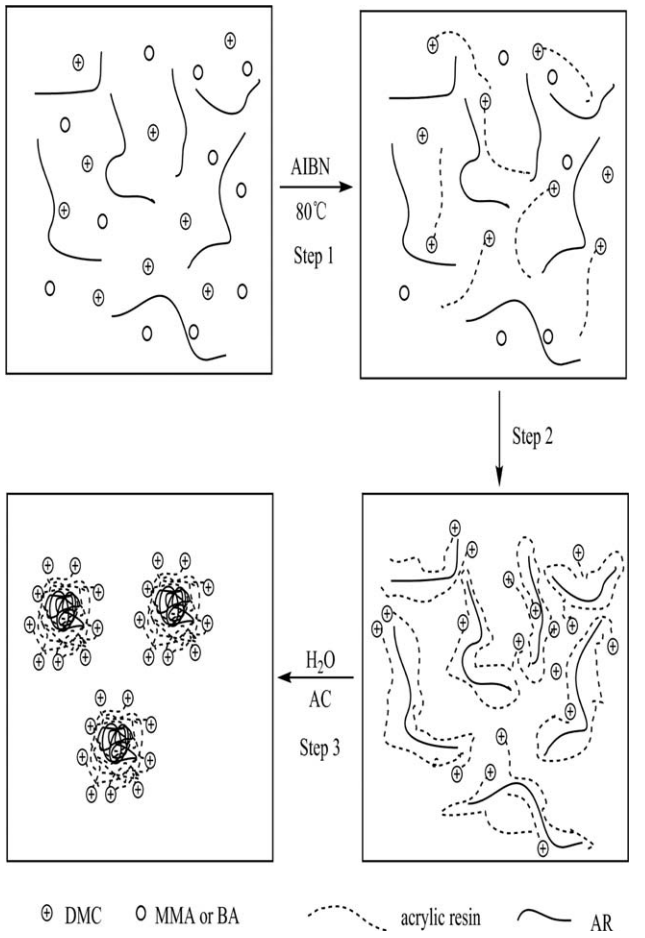

Figure 2. The experimental mechanism scheme for the CPAAR emulsions.

Rheology Measurement

The rheological properties of the dispersions were analyzed in a TA Instrument AR2000ex rheometer. All tests were carried out at 25°C with a DIN concentric cylinders geometry. The diameters of the rotating rod and static cylinder were 28 and 30 mm, respectively. Strain (γ amplitude experiments (0.01 to 100%) were performed at a frequency of 0.1 Hz to determine the linear viscoelastic region. Then frequency sweeps (0.1 to 100 Hz) were performed with a strain of 1% at 25°C. All of the samples were loaded into the rheometer measurement cup and allowed to equilibrate at 25°C for 5 min, and then, the samples underwent a constant shearing treatment (1 $s^{-1}$for 10 min) before analysis to remove history effects.

Particle Size and Micromorphology Measurement

The particle size and dispersivity index (DPI) of CPAAR dispersions were analyzed by Nano-ZS dynamic light scattering (Malvern, United Kingdom). Its morphology was observed by Hitachi (H-600) TEM instrument. The concentration used for dynamic light scattering and TEM measurements was 10 g L^{-1}. All of the samples were dispersed by a sonicator before the analysis.

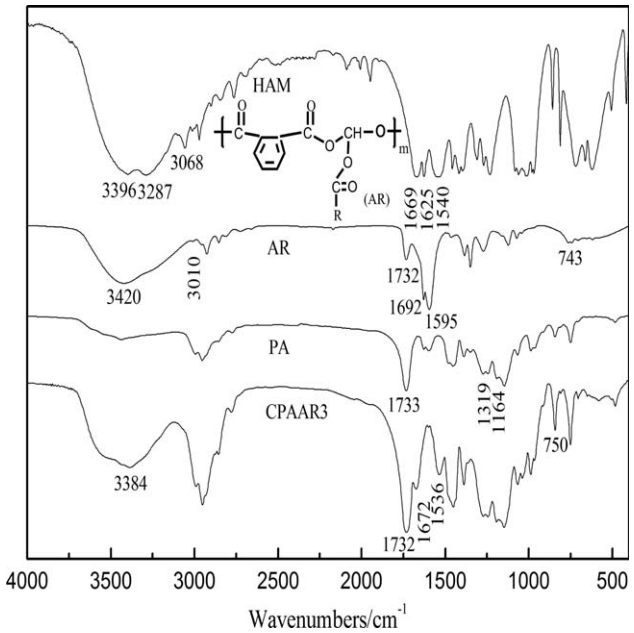

Figure 3. The FTIR spectrum of HAM, AR, PA, and CPAAR3.

Contact Angle and Surface Free Energy of Films

The contact angle of CPAAR films was measured with a JJC-I contact angle goniometer (Changchun Optical Instrument Company, China) at 25°C and the reported results were the mean values of five replicates. The preferable equation to calculate the interfacial tension, which was also surface free energy between polymers and an ordinary liquid, was as follows[24]:

$$(1 + \cos\theta_{liquid})\gamma_{liquid} = 4\left(\frac{\gamma^d_{liquid}\gamma^d}{\gamma^d_{liquid} + \gamma^d} + \frac{\gamma^p_{liquid}\gamma^p}{\gamma^p_{liquid} + \gamma^p}\right) \quad (1)$$

where γ liquid was the surface tension of wetting liquid and γ^P, γ^d were dispersive and polar component, respectively. θ_{liquid} was water or ethylene glycol contact angle of the polymer. γ^d and γ^P for latex films could be calculated by substituting values for water and ethylene glycol into eq. (1) and solving the corresponding set of simultaneous equations. The total surface energy γ was the summation of γ^d and γ^P. The γ^d_{liquid} and γ^P_{liquid} for water were 22.1 and 50.7 mJ m^{-2} and for ethylene glycol were 31.0 and 48.2 mJ m^{-2}, respectively.

Water Absorption of Films

Water absorption (WA) of copolymer films was calculated by the formula $WA = (m_2 - m_1)/m_1 \times 100\%$, in which, m_1 was the quality of dried films and m_2 was the quality of immersed films. The film samples were cut into 30 × 30 mm^2 and immersed in a weighing bottle with distilled water standing for 24 h at room temperature; then they were taken out and the films were weighted after the surface moisture were absorbed by a filter paper. The operations were repeated until the constant weight (m_2) was achieved. Then wet samples were dried under reduced pressure for 24 h at 100°C and weighted (m_1).

RESUITS AND DISCUSSION

Structural Characteristics

The structures of HAM, AR, PA (P(DMC/MMA/BA)), and CPAAR3 were characterized by FTIR spectroscopy. As shown in Figure 3, several features indicated the occurrence of interaction between HAM, PA and AR.

In the spectrum of HAM, the peaks at 3396 and 1540 cm^{-1} could be ascribed to the stretching vibration[25,26] and blending vibration of —NH group, respectively. The peak at 3287 cm^{-1} was corresponding to —OH group in HAM. The characteristic peaks of —NH and —OH groups were also observed in FTIR spectrum of CPAAR3. It suggested the successful incorporation of HAM into the CPAAR3 chains.

As shown in the AR spectrum, the peak at 3420 cm^{-1}could be attributed to the stretching vibration of —OH group. The peak at 1595 and 743 cm^{-1} represented stretching vibration and breathing vibration of the aromatic structure in AR.[2,4] The characteristic peaks of —OH group and aromatic structure were also detected in CPAAR3 spectrum.

In comparison of AR and PA spectra, the width and intensity of —OH group in the CPAAR3 spectrum increased. This phenomenon suggested that HAM was successfully incorporated into the CPAAR chains. In addition, compared with HAM, AR, and PA spectra, the intensity of the absorption peak of the C═O group in the CPAAR3 spectrum was obviously enhanced. Therefore both indicated the CPAAR3 consisted of HAM, AR, and PA.

Particle Size and Morphology

The effect of HAM content on the particle size and dispersivity index (DPI) of the emulsions was analyzed by dynamic light scattering. As shown in Figure 4 and Table II, the Z-average particle size of the dispersions deceased from 107.7 to 92.2 nm as well as the corresponding DPI from 0.126 to 0.117 as HAM content increased from 0 to 4.9 wt %. And then with further increasing HAM content, particle size increased. The hydrophilicity of polymer surface increased with the initial addition of HAM as a nonionic monomer. And simultaneously the Gibbs free energy and interfacial tension decreased between polymer surface and water.[27,28] Therefore smaller particles size formed as a result of increased number of latex particle under the same shear force. Meanwhile, the stronger hydrogen bond force among polymer chains contributed to closer aggregation of molecular chains caused by increasing amino and hydroxyl groups in HAM structure. As a result, particles size decreased.[29] However, as HAM content was more than 4.9 wt %, the viscosity increased remarkably due to intensive crosslinking,[30] and particles size increased.

The emulsions of CPAAR0, CPAAR1, CPAAR2, and CPAAR3 were dyed with phosphotungstic acid. As shown in Figure 5, in contrast of the CPAAR0, CPAAR2, and CPAAR3 particles morphology, the CPAAR1 particles displayed a particle morphology with a relative uniform particle size distribution at the same concentration of 10 g L^{-1}. The results were in agreement with the particle size results obtained by the light-scattering technique. The irregular particle morphology could be explained by (1) lack of adequate hydrophilicity with <4.9 wt % HAM addition; (2) homopolymer of HAM as addition of HAM was more than 4.9 wt %.

Table II. Particle Size and Dispersivity Index Results of CPAAR Emulsions with Different HAM Content

Sample	HAM content (%)	Diameter (nm)	DPI
CPAAR0	0	107.7	0.126
CPAAR1	4.9	92.2	0.117
CPAAR2	9.8	226.2	0.154
CPAAR3	14.7	351.1	0.176
CPAAR4	19.6	426.5	0.203

Freeze-Thaw Stability Measurement of Emulsion

The freeze-thaw stability of waterborne emulsion was a very important characteristic, which determined their safe storage period and practical application condition, especially in some cold regions. The percentage of HAM had great influence on freeze-thaw stability of hybrid emulsions, which was characterized by particle size, dispersivity index (DPI) and zeta potential value of the emulsions. The result suggested that the freeze-thaw stability of CPAAR0, CPAAR2 and CPAAR4 emulsion was satisfactory, as shown in Figure 6 and Table III. The particle size and DPI of CPAAR0 emulsion only increased by 19.7 and 0.037 nm, respectively, after five cycles while that of CPAAR2 and CPAAR4 emulsion increased by 39 nm, 0.083 and 44.6 nm, 0.109, suggesting stability of CPAAR emulsion decreased with increasing content of HAM. The results were further confirmed by zeta potential value. The zeta potential values of CPAAR0, CPAAR2, and CPAAR4 emulsion decreased by 2.7, 3.5, and 4.6 mV, respectively, after five cycles, as shown in Table III. As known, the zeta potential was measured by examining the electric charges exposed in the outermost particles, which were the so-called effective charges that influenced zeta potential values. A higher zeta potential value meant a stronger electrostatic repulsive energy of the particle surface, which inhibited aggregation of colloidal particle. Thereby the stability of the emulsions decreased, as zeta potential value decreased. With addition of HAM content, on one hand, the viscosity of emulsions further increased during ice crystal nucleation. Therefore the thaw process of colloidal dispersion became difficult, resulting in bigger particle size. On the other hand, particle-particle interactive forces increased due to crosslinking of HAM, which inhibited recovery of polymer chains during thaw process.[18] This was also confirmed by rheological behavior of CPAAR emulsions. In addition, the increased hydration layer around polymer particle due to hydrophilicity of HAM aggravated ice crystal nucleation in frozen progress, which was adverse to recovery of polymer chains in thaw progress.[31] As a result, the particle size and DPI increased. The increased DPI indicated the aggregation and coagulum of colloidal particle took place in a certain during the freeze-thaw process, which resulted in a irregular distribution of colloidal particle, as freeze-thaw cycle number increased.

Rheological Behavior of CPAAR Emulsions

The apparent viscosity as a function of shear rate for CPAAR emulsions with different HAM content was shown in Figure 7. As shown in Figure 7, the viscosity of emulsions increased with increasing HAM content. With increasing crosslinking density

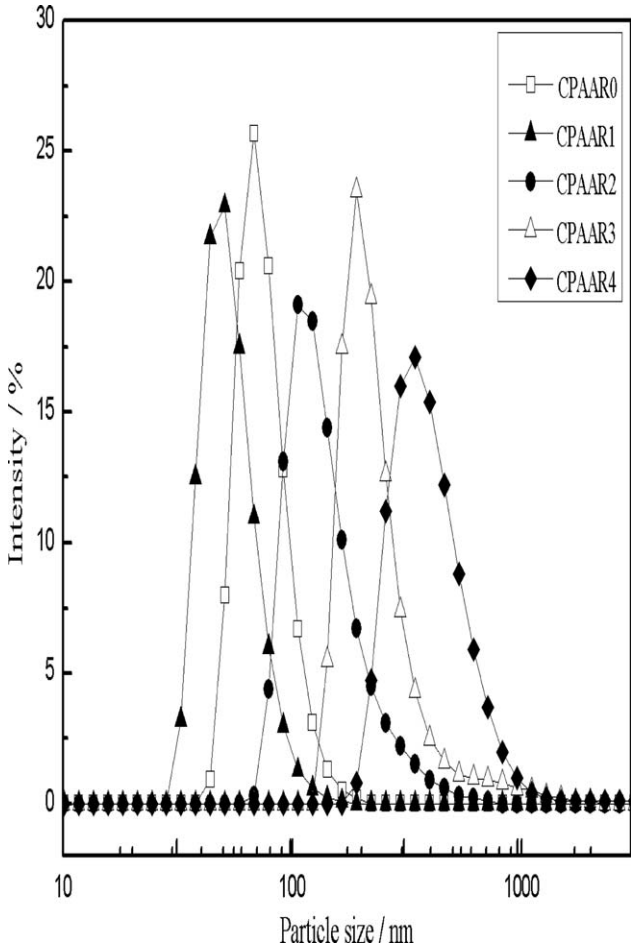

Figure 4. Particle size of CPAAR emulsion with different HAM content.

in the polymer chains, the motion of molecular chains was hindered by C—O—O bonds and hydrogen bonds. Therefore the apparent viscosity increased. In addition, with increasing hydrophilicity due to the introduction of HAM as nonionic monomer, the volume of hydration layer increased, which was also adverse to the motion of the molecular chains. Consequently, the viscosity increased.[15]

Meanwhile, the viscosity of CPAAR0 and CPAAR1 emulsions kept almost invariable while the viscosity of CPAAR2, CPAAR3, and CPAAR4 emulsions decreased with increasing shear rate, which suggested that CPAAR emulsions in the HAM content range of 0 and 4.9 wt % presented as Newtonian fluids while presented as pseudoplatic fluids in the HAM content range of 9.8, 14.7, and 19.6 wt %. This phenomenon also indicated the CPAAR emulsions transferred from Newtonian fluids to pseudoplatic fluids with increasing HAM content.[32,33] With addition of HAM, which contained crosslingking groups-hydroxymethyl groups and acylamino groups, the C—O—C bonds and hydrogen bonds formed among latex particles, as shown in Figure 8. Consenquently, the crosslinking density of molecular chains increased. At the same time, the hydrogen-bond interaction and thickness of colloidal hydration layer also increased. The entanglement and hydrogen-bond interaction of molecular chains were impaired as shear rate increased. Therefore the viscosity of

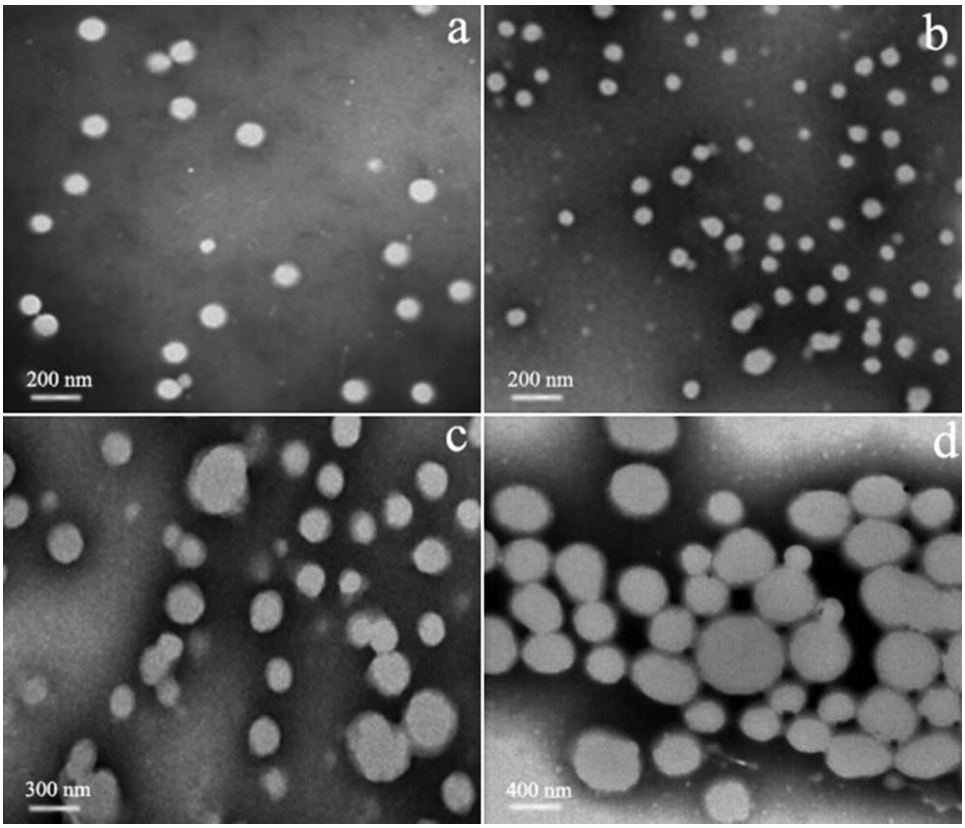

Figure 5. TEM of CPAAR0 (a), CPAAR1 (b), CPAAR2 (c), and CPAAR3 (d) emulsions.

CPAAR2, CPAAR3, and CPAAR4 emulsions decreased and these emulsions presented as shear shining behavior. Obviously, the viscosity of CPAAR4 emulsions was almost constant at lower shear rate and decreased at higher shear rate. This phenomenon could be explained by pronounced crosslinking interaction and hydrogen-bond interaction of molecular chains, which was induced by excessive HAM content.

Oscillatory measurements offered a nearly non-destructive measuring method, which allowed structural studies on complex systems. Studies on the viscoelastic properties of polymer fluids have long been known. Figure 8 described the storage modulus (G') and the loss modulus (G'') of CPAAR emulsions with different HAM content (carried out in the linear viscoelastic region at $\gamma = 1\%$). The storage modulus quantifies the mechanical properties of the respective emulsions.

As shown in Figure 9, both G' and G'' of CPAAR emulsions increased with increasing addition of HAM, which was in agreement with the theory that in general, most emulsions have an internal network structure resulting from intermolecular interactive forces. For CPAAR0 emulsion, the emulsion behaved like viscous liquid, showing G' was lower than G'' over the whole frequency range. CPAAR2 emulsion displayed as a viscoelastic liquid, since G' was lower than G'' in the lower frequency range and G' became equal to G'' in the higher frequency range, indicating that the elasticity of CPAAR2 emulsion was sensitive to rapid movement and the physical junctions in the networks started to be broken down in the higher frequency range. CPAAR4 emulsion was gel-like characterized by the fact that G' was almost equal to G'' in whole frequency range and the corresponding loss factor ($\tan \delta = G''/G'$) was equal to 1, suggesting

Table III. The Results from Freeze-Thaw Stability of CPAAR0 (a), CPAAR2 (b), and CPAAR4 (c)

Sample	Diameter (nm)	DPI	Cycle number	Zeta potential (mV)
CPAAR0	114.7	0.146	1	44.8
	116.3	0.151	2	44.1
	117.2	0.176	3	43.5
	118.5	0.180	4	42.8
	134.4	0.183	5	42.1
CPAAR2	236.7	0.171	1	40.6
	246.8	0.203	2	39.1
	258.3	0.215	3	38.5
	266.8	0.241	4	37.3
	275.7	0.254	5	37.1
CPAAR4	436.5	0.214	1	36.9
	448.8	0.272	2	35.5
	450.9	0.291	3	34.7
	457.6	0.317	4	33.1
	481.1	0.323	5	32.3

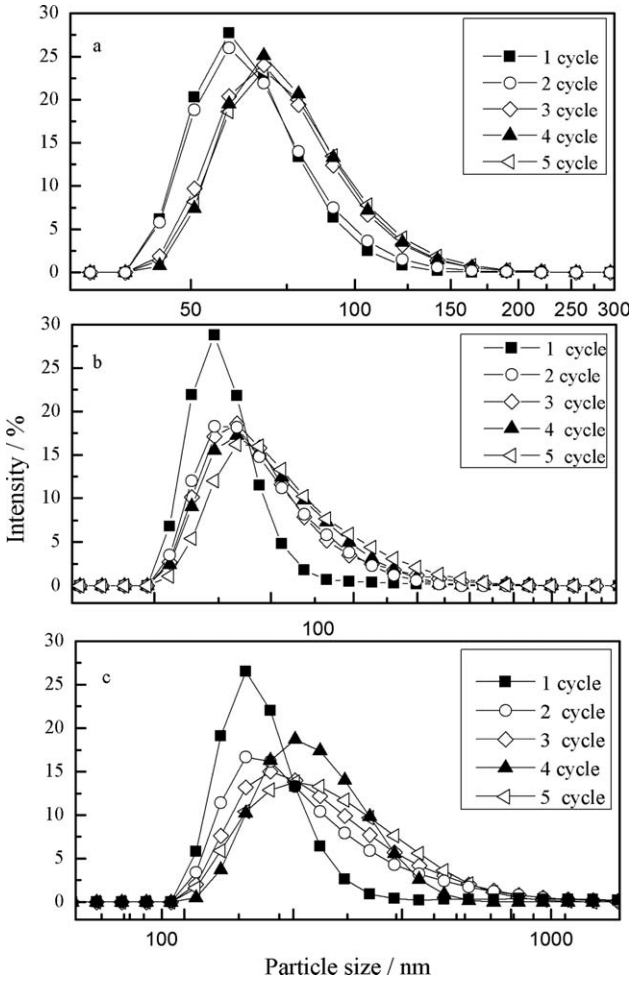

Figure 6. Freeze-thaw stability of CPAAR0 (a), CPAAR2 (b), and CPAAR4 (c) emulsion.

that CPAAR4 emulsion under study showed good tolerance to external forces in the frequency range. It was explained that there were permanent physical junctions in CPAAR4 emulsion,[34] which inhibited the destruction of colloidal structure due to increased crosslinking density with addition of HAM. Therefore, the addition of HAM would make for the improvement of the elasticity of CPAAR emulsions.

Thermal Properties

Figure 10 and Table IV showed TG and DTG results of the CPAAR films with different HAM content. The thermal stability was evaluated by the degradation temperature at 5 wt % weight loss ($T_{d,\ 5\%}$), 50 wt % weight loss ($T_{d,\ 50\%}$) and maximum degradation temperature (T_{max}), which were summarized in Table II. As to CPAAR films, there were two stages under degradation process. The first stage, from 190.5 to 280.4°C, was attributed to the breaking of ester in acrylic and alkyd chains.[1] The second stage, from 298.6 to 451.2°C, was mainly ascribed to the cleavage of C—C linkages in the acrylic and alkyd structure.[35]

At the same time, it was observed that HAM content played an important role in the high-temperature thermal stability. The degradation temperature at a 5% weight loss increased from 198.48 to 229.07°C as the HAM content increased from 0 to

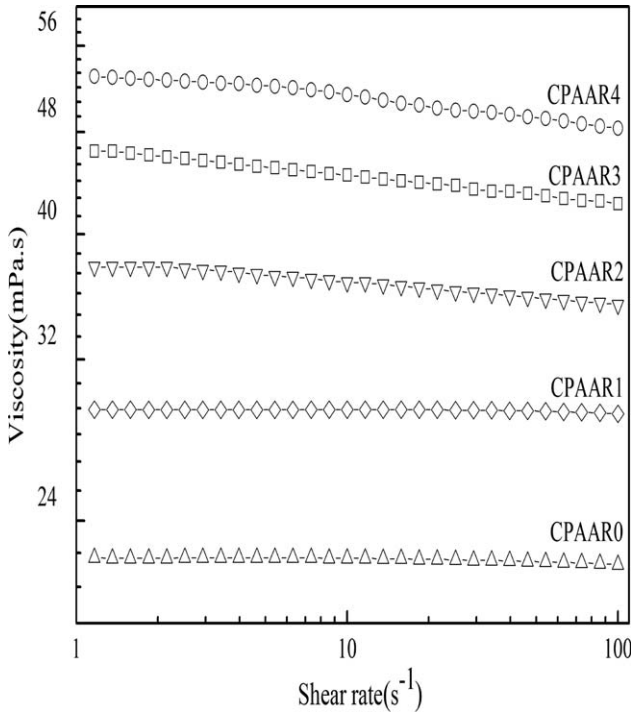

Figure 7. Viscosity versus shear rate of the CPAAR emulsions with different HAM content.

19.6 wt %. A similar phenomenon was detected for degradation temperature at a 50% weight loss. In addition, the main degradation peak of CPAAR films shifted to higher temperature, with the maximum degradation temperature at 360.82, 367.15, 378.57, 385.63, and 393.86°C in the second stage. The behavior could be attributed to the increasing crosslinking degree and rigidity of molecular chain with the introduction of HAM.[35]

Water Absorption and Surface Free Energy

Table V showed water absorption, contact angle and surface free energy (γ was calculated from contact angle with water and ethylene glycol) of the films. As HAM content increased from 0 to 4.9 wt %, the water absorption increased by 4.42%, and the

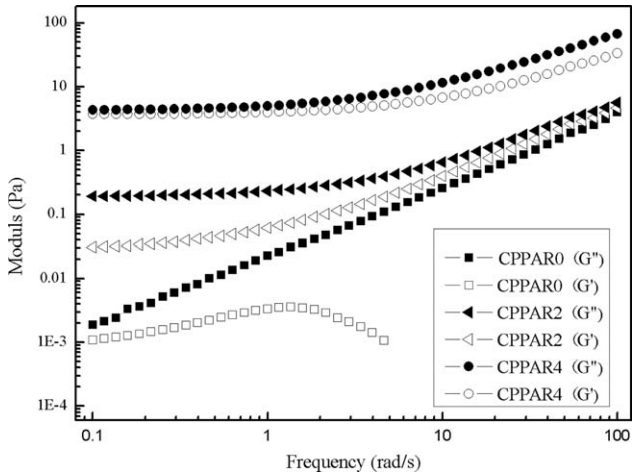

Figure 8. Modulus versus frequency of the CPAAR emulsions with different HAM content.

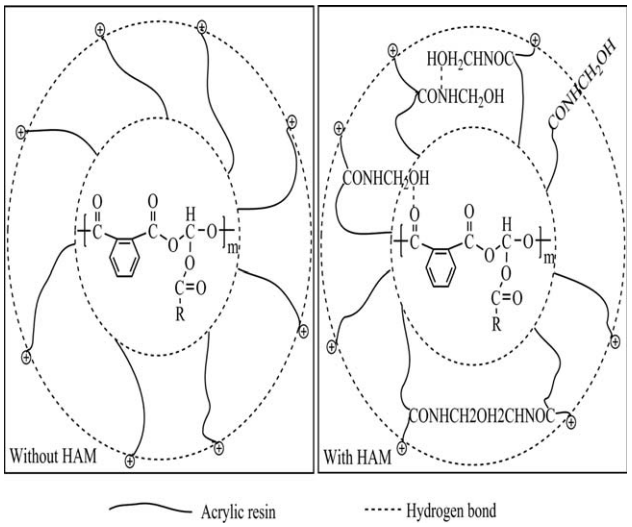

Figure 9. The schematic for crosslinking mechanism of HAM.

corresponding contact angle with water and ethylene glycol decreased by 5.64° and 3.63°, respectively, which resulted in a similar phenomenon for surface free energy of films. However, as HAM content increased further, there was little variation in water absorption, contact angle with water or ethylene glycol and surface free energy. The reasons of these phenomena

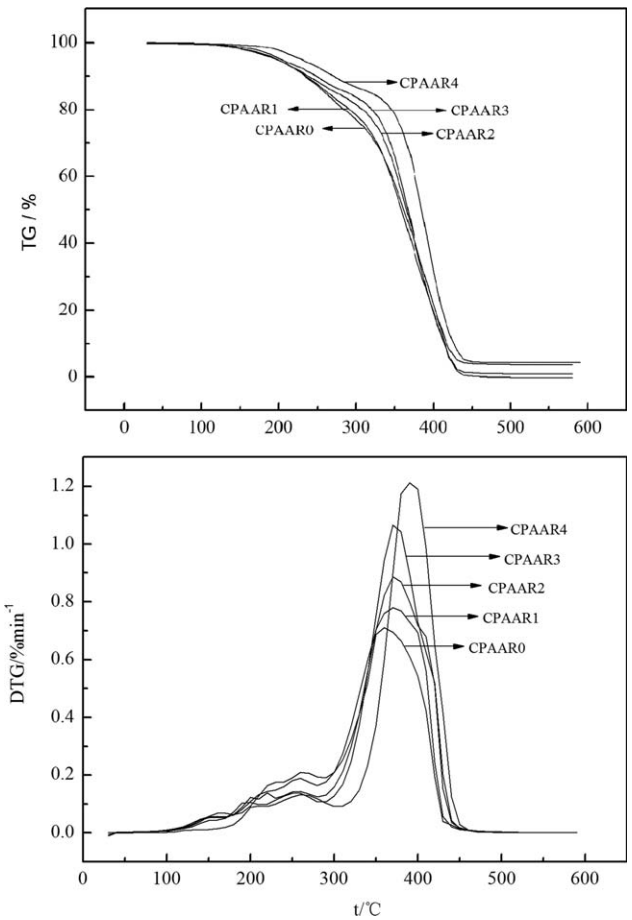

Figure 10. TG-DTG curve of CPAAR films with different HAM content.

Table IV. TG-DTG Results of Cationic Acrylic/Alkyd Resin Emulsions with Different HAM Content

Sample	TG		DTG
	$T_{d,\ 5\%}$ (°C)	$T_{d,\ 50\%}$ (°C)	T_{max} (°C)
CPAAR0	198.48	362.19	260.13, 360.82
CPAAR1	208.09	369.14	258.36, 367.18
CPAAR2	208.22	375.81	259.64, 378.57
CPAAR3	213.04	377.55	259.61, 385.63
CPAAR4	229.07	385.00	259.75, 393.86

involved in augment of hydrophilic units in the copolymer. The results demonstrated that there would appear more hydrophilic groups on surface of the films, which contributed to a lower interfacial tension and a better compatibility between polymer surface and water with <4.9 wt % amount of HAM.[4,36] Therefore the corresponding surface free energy increased. But with further increasing HAM content, more network structure formed due to increasing crosslinking density. Consequently, water molecules were hard to penetrate into membranes, resulting in a constant water absorption and surface free energy. The explanation was supported by the fact that there were the similar phenomenon in dispersion component (γ^d) and polar component (γ^p) in the whole process.[37,38]

CONCLUSIONS

A series of cationic acrylic/alkyd hybrid emulsions (CPAAR) were successfully prepared by surfactant-free emulsion polymerization, incorporating nonionic groups of hydroxymethyl acrylamide (HAM) of different content to CPAAR backbone and using methacryloxyethyltrimethyl ammonium chloride, methyl methacrylate, butyl acrylate and alkyd resin as reaction monomers. The result of FTIR spectroscopy ascertained the presence of HAM in the CPAAR chains. The result of particles size indicated the CPAAR emulsion with 4.9 wt % HAM displayed smallest average particle size of 92.2 nm. This was confirmed by transmission electron microscopy (TEM) morphology, which showed that the CPAAR emulsion with 4.9 wt % HAM particles displayed a particle morphology with a relative uniform particles size distribution at the concentration of 10 g L^{-1}. In addition, freeze-thaw stability of emulsion was characterized by particle size analyzer, which showed particle size and dispersivity index (DPI) of emulsion without HAM increased by 19.7 and 0.037 nm while that of emulsion with 19.6 wt % HAM increased by 44.6 and 0.109 nm after five cycles. Therefore freeze-thaw stability of emulsion decreased as addition of HAM increased. The result was further confirmed by zeta potential value. The steady rheology of CPAAR emulsions suggested that initial viscosity of the emulsions increased from 22.48 to 53 mPa s^{-1} and the emulsions transferred from Newtonian fluid to pseudoplastic fluid, as HAM content increased from 0 to 19.6 wt %. Oscillatory measurements showed the addition of HAM would make for the improvement of the elasticity of CPAAR emulsions. At the same time, the TG-DTG showed the degradation temperature at 5% weight loss increased by 30.59°C. In

Table V. Water Absorption, Contact Angle, and Surface Free Energy of the Film with Different HAM Content

		Contact angle (°)		Surface free energy (mJ m^{-2})		
Sample	WA (%)	Water	Ethylene glycol	γ^d	γ^p	γ
CPAAR0	4.56	85.98	44.21	24.67	9.58	34.25
CPAAR1	8.98	80.34	40.58	27.42	11.85	39.27
CPAAR2	9.78	81.56	41.19	28.87	12.58	41.45
CPAAR3	10.21	82.18	42.16	29.36	13.42	42.78
CPAAR4	10.59	82.69	42.23	29.74	13.82	43.56

addition, water absorption and the corresponding surface free energy of films increased by 4.42% and 5.02 mJ m^{-2}, respectively with addition of HAM from 0 to 4.9 wt %. However, the water absorption and surface free energy kept almost invariable with further increase in HAM content.

ACKNOWLEDGMENTS

The authors express sincere thanks to National Science Foundation of China (Grant No. 21204046 and 51373091), Project-Sponsored by SRF for ROCS, SEM and Shaanxi Province Science and Technology Research and Development Program of China (Grant No. 2013KJXX-77).

REFERENCES

1. Pronob, G.; Monalisha, B.; Chandramika, B.; Swapan, K. D. *Prog. Org. Coat.* **2014**, *77*, 87.
2. Tsavalas, J. G.; Luo, Y.; Schork, F. J. *J. Appl. Polym. Sci.* **2003**, *87*, 1825.
3. Hamersveld, E. M. S.; van Es, J. J. G. S.; Cruppers, F. P. *Colloids Surf. A Physicochem. Eng. ASP* **1999**, *153*, 285.
4. Nartin, T.; Kent, R. M.; Mark, D. S. *Prog. Org. Coat.* **2012**, *73*, 425.
5. Roque, J. M.; Monika, G.; Itxaso, B.; Maria, P.; Maria, J. B.; Jose, M. A. *Polymer* **2009**, *50*, 5892.
6. Nabuurs, T.; Baijards, R. A.; German, A. L. *Prog. Org. Coat.* **1996**, *27*, 163.
7. Pirita, U.; Nina, H.; Pekka, M.; Sirkka, L. M.; Salme, K. *Prog. Org. Coat.* **2008**, *63*, 92.
8. Nina, H.; Saila, J.; Leena, P.; Salme, K. *Prog. Org. Coat.* **2010**, *67*, 329.
9. Wang, C.; Jones, F. N. *J. Appl. Polym. Sci.* **2000**, *78*, 1698.
10. Holmberg, K. *Prog. Org. Coat.* **1992**, *20*, 325.
11. Abdel-Mohsen, F. F.; Abdel-Hamed EI-Zayar, S. *Surf. Coat. Int.* **1992**, *75*, 349.
12. Jowkar-Deriss, M.; Karlsson, O. J. *Prog. Colloid. Polym. Sci.* **2003**, *124*, 149.
13. Jowkar-Deriss, M.; Karlsson, O. J. *Colloids Surf. A* **2004**, *245*, 115.
14. Colombini, D.; Jowkar-Deriss, M.; Karlsson, O. J.; Maurer, F. *Macromolecules* **2004**, *37*, 2596.
15. Mongi, E.; Sani, B. *J. Indus. Eng. Chem.* **2013**, *1788*, 1.
16. Mongi, E.; Ayman, B. M.; Sami, B. *Prog. Org. Coat.* **2014**, *12*, 1.
17. Herng, D. H.; Yu, D. L. *Polymer* **2000**, *41*, 5695.
18. Monika, G.; Roque, J. M.; Itxaso, B.; Maria, P.; Maria, J. B.; Jose, M. A. *Polymer* **2010**, *20*, 5313.
19. Jamie, D.; Mark, D. S. *Prog. Org. Coat.* **2012**, *73*, 330.
20. Amie, D.; Venkat, D.; Mark, D. S. *Prog. Org. Coat.* **2012**, *73*, 308.
21. Do, I. L. *Polymer* **2005**, *46*, 1287.
22. Wang, C.; Li, X. R.; Du, B.; Li, P. Z.; Mi, X. H. *J. Polym. Res.* **2013**, *20*, 94.
23. Richard, J. E.; James, E. D.; Dave, E. S.; Loek, W. *Prog. Org. Coat.* **1999**, *36*, 45; 396:83.
24. Julio, C. C.; Miriam, C. S.; Cecilia, I. A. I. *React. Funct. Polym.* **2013**, *71*, 440.
25. Abdirahman, S.; Dominique, M. R. G.; Andrew, G. M. *React. Funct. Polym.* **2010**, *70*, 230.
26. Wang, R. M.; Wang, J. F.; Wang, X. W.; He, Y. F.; Zhu, Y. F.; Jiang, M. L. *Prog. Org. Coat.* **2011**, *71*, 369.
27. Edwin, A. M.; Betty, L. L. *Prog. Org. Coat.* **2011**, *72*, 731.
28. Guillaume, T.; Bernard, B.; Bruno, A. *Prog. Polym. Sci.* **2011**, *36*, 191.
29. Narin, T. K.; Mark, D. S. *Prog. Org. Coat.* **2012**, *73*, 382.
30. Evelyne, V. R.; Ed, B. M.; Dimitris, V.; Gao, H. F. *Eur. Polym. J.* **2011**, *47*, 746.
31. Gumfekar, S. P.; Kunte, K. J.; Ramjee, L.; Kate, K. H.; Sonawane, S. H. *Prog. Org. Coat.* **2011**, *72*, 632.
32. Wang, H. H.; Zou, J.; Shen, Y. D.; Fei, G. Q.; Mou, J. *J. Appl. Polym. Sci.* **2013**, *130*, 1.
33. Matthew, P. C.; Taigyoo, P.; Timothy, E. L. *J. Adhes.* **2009**, *85*, 1.
34. Yang, T. T.; Peng, H.; Cheng, S. Y.; Park I. J. *J. Fluor. Chem.* **2005**, *126*, 1570.
35. Fu, Z. H.; Zhang, N.; Liu, J.; Li, T. S.; Xu, W. J.; Wang, F.; Wang, T.; Zhai, Z.; Liu, L. L.; Mao, L. Y.; Wu, Y. J. *J. Colloid. Interf. Sci.* **2013**, *94*, 409.
36. Wang, C.; Li, X. R.; Du, B.; Li, P. Z.; Li, H. B. *Carbohydr. Polym.* **2013**, *95*, 637.
37. Xin, H.; Shen, Y. D.; Li, X. R. *Colloids Surf. A Physicochem. Eng. ASP* **2011**, *384*, 205.
38. Zhou, J. H.; Zhang, L.; Ma, J. Z. *Chem. Eng. J.* **2013**, *223*, 8.